JOURNAL OF VIROLOGY, Mar. 2006, p. 2684–2693 Vol. 80, No. 6
0022-538X/06/$08.00+0 doi:10.1128/JVI.80.6.2684–2693.2006

Modeling the Early Events of Severe Acute Respiratory Syndrome Coronavirus Infection In Vitro

Yu-Ting Yen,[1] Fang Liao,[2] Cheng-Hsiang Hsiao,[3] Chuan-Liang Kao,[4] Yee-Chun Chen,[5] and Betty A. Wu-Hsieh[1]*

Graduate Institute of Immunology[1] and Graduate Institute of Clinical Laboratory Sciences and Medical Biotechnology,[4] National Taiwan University College of Medicine, Department of Pathology[3] and Department of Internal Medicine,[5] National Taiwan University Hospital, and Institute of Biomedical Sciences, Academia Sinica,[2] Taipei, Taiwan

Received 13 September 2005/Accepted 15 December 2005

The clinical picture of severe acute respiratory syndrome (SARS) is characterized by pulmonary inflammation and respiratory failure, resembling that of acute respiratory distress syndrome. However, the events that lead to the recruitment of leukocytes are poorly understood. To study the cellular response in the acute phase of SARS coronavirus (SARS-CoV)–host cell interaction, we investigated the induction of chemokines, adhesion molecules, and DC-SIGN (dendritic cell-specific ICAM-3-grabbing nonintegrin) by SARS-CoV. Immunohistochemistry revealed neutrophil, macrophage, and CD8 T-cell infiltration in the lung autopsy of a SARS patient who died during the acute phase of illness. Additionally, pneumocytes and macrophages in the patient's lung expressed P-selectin and DC-SIGN. In in vitro study, we showed that the A549 and THP-1 cell lines were susceptible to SARS-CoV. A549 cells produced CCL2/monocyte chemoattractant protein 1 (MCP-1) and CXCL8/interleukin-8 (IL-8) after interaction with SARS-CoV and expressed P-selectin and VCAM-1. Moreover, SARS-CoV induced THP-1 cells to express CCL2/MCP-1, CXCL8/IL-8, CCL3/MIP-1α, CXCL10/IP-10, CCL4/MIP-1β, and CCL5/RANTES, which attracted neutrophils, monocytes, and activated T cells in a chemotaxis assay. We also demonstrated that DC-SIGN was inducible in THP-1 as well as A549 cells after SARS-CoV infection. Our in vitro experiments modeling infection in humans together with the study of a lung biopsy of a patient who died during the early phase of infection demonstrated that SARS-CoV, through a dynamic interaction with lung epithelial cells and monocytic cells, creates an environment conducive for immune cell migration and accumulation that eventually leads to lung injury.

Severe acute respiratory syndrome (SARS) in adults causes new pulmonary infiltration, lymphopenia, thrombocytopenia, and high levels of proinflammatory cytokines and chemokines (30) and C-reactive protein (28) in the sera. The clinical picture is characterized by a cascade of immunological events leading to pulmonary inflammation and respiratory failure (9, 17), resembling adult acute respiratory distress syndrome (ARDS) (8). High levels of chemokines and cytokines, triggered by the host immune response to SARS coronavirus (SARS-CoV), are believed to contribute to the progressive pulmonary infiltration of macrophages (16), polymorphonuclear leukocytes (2), and T cells (11) and to eventual diffuse alveolar damage and fibrosis (12). However, it remains to be determined how the cellular response in the early stage of virus-host cell interaction results in the sequence of events that leads to the severe clinical outcome.

In situ hybridization and immunohistochemistry revealed that both SARS-CoV nucleic acids and antigens are present within type II pneumocytes (26). Alveolar macrophages are also reported to harbor SARS-CoV (23). Hence, it is important to investigate how the interaction between SARS-CoV and pneumocytes and macrophages influences the subsequent events in the lung.

DC-SIGN (dendritic cell-specific ICAM-3-grabbing nonintegrin) is a type II C-type lectin that is naturally expressed in human dendritic cells. It has been reported that DC-SIGN binds SARS-CoV and mediates its entry into myeloid dendritic cells by binding to the spike protein (31). However, the inducibility of DC-SIGN in cells encountering the virus and its significance in SARS-CoV infection in vivo have not been reported.

In this study, we detected neutrophils, macrophages, and T cells and the expression of adhesion molecules and DC-SIGN in the lung of a patient in the acute phase of SARS. After screening a panel of epithelial and monocytic cell lines, we found that A549 and THP-1 cells were susceptible to SARS-CoV. By employing A549 and THP-1 cells in in vitro assay systems, we compared the responses of both lung epithelial cells and monocytic cells to SARS-CoV and to CoV-229E. Based on our results, we propose a two-wave model to explain how cellular infiltration may result in SARS: (i) pulmonary epithelial cells infected by SARS-CoV express adhesion molecules and produce high levels of CCL2/monocyte chemoattractant protein 1 (MCP-1) and CXCL8/interleukin-8 (IL-8) which recruit macrophages and neutrophils, and (ii) macrophages recruited by CCL-2/MCP-1 interact with SARS-CoV and produce a set of chemokines that attract more monocytes and neutrophils as well as activated T cells. Moreover, we demonstrated in vitro that DC-SIGN is inducible in lung epithelial and monocytic cells after SARS-CoV infection. Importantly, in vivo DC-SIGN expression in macrophages and pneumocytes is demonstrable in the acute respiratory phase of SARS-CoV infection.

* Corresponding author. Mailing address: Graduate Institute of Immunology, College of Medicine, National Taiwan University, No. 1 Jen-Ai Road, Section 1, Taipei 10051, Taiwan. Phone: 886-2-23123456, ext. 8630. Fax: 886-2-23217921. E-mail: wuhsiehb@ha.mc.ntu.edu.tw.

MATERIALS AND METHODS

Immunohistochemistry. Autopsy lung specimens were taken from a SARS-CoV-infected patient admitted to National Taiwan University Hospital who died of myocardial infarction on the 7th day after admission. Paraffin-embedded tissues were sectioned, deparaffinized, and rehydrated. The sections were first treated with Trilogy retrieval buffer (Cell Marque Cooperation, Austin, TX) in steam heat for 20 min, followed by treatment with 0.3% hydrogen peroxide. To phenotype the infiltrating cells, polyclonal rabbit anti-human CD3 antiserum (1:100; DAKO USA, Carpinteria, CA), monoclonal mouse anti-human CD68 antibody (clone PG-M1, 1:200; DAKO), and monoclonal mouse anti-human CD8 antibody (clone IA5, 1:200; BioGenex, San Ramon, CA) were used. To detect SARS-CoV antigen, the sections were stained with polyclonal mouse anti-SARS-CoV antiserum (1:1,000; kindly provided by M. F. Chang, National Taiwan University) (9) at 4°C overnight. After incubation, the slides were sequentially stained in a Nexis autostainer (Ventana, Tucson, AZ) with the reagents provided in the Ventana basic alkaline phosphatase red detection kit (Ventana) and counterstained with hematoxylin.

To detect P-selectin or DC-SIGN, tissue sections were pretreated with antigen retrieval buffer (pH 10) (AR10; BioGenex) and Trilogy retrieval buffer in sequence in steam heat, followed by hydrogen peroxide treatment at 4°C overnight. After incubation with anti-P-selectin antibody (C20, 1:100; Santa Cruz Biotech., Santa Cruz, CA) or anti-DC-SIGN antibody (monoclonal antibody [MAb] 161; R&D Systems, Minneapolis, MN) at 4°C overnight, the slide was incubated with biotin-labeled donkey anti-goat antibody at 37°C for 20 min. A biotin-streptavidin detection system and the Ventana iView diaminobenzidine detection kit (Ventana) were used for color development, and counterstaining was with hematoxylin.

Cell lines. The NCI-H292 human pulmonary mucoepidermoid carcinoma cell line, the A549 human pulmonary adenocarcinoma cell line, and the NL-20 immortalized epithelial lung cell line were purchased from the American Type Culture Collection (ATCC) (Manassas, VA). NCI-H292 and NL-20 cells were grown in RPMI 1640 supplemented with 10% heat-inactivated fetal bovine serum (FBS) under 5% CO_2 at 37°C. A549 cells were grown in Ham's F12K with 2 mM L-glutamine and 1.5 g/liter sodium bicarbonate supplemented with 10% heat-inactivated FBS.

The THP-1 human monocytic cell line and the HL-CZ human acute promyelocytic leukemia cell line (ATCC) were maintained in Dulbecco's modified Eagle medium (BioWhittaker, Walkersville, MD) supplemented with 10% heat-inactivated FBS. The WBC 264-9C cell line (ATCC; a macrophage-like cell line derived by fusion of normal human peripheral blood leukocytes with the mouse RAW 264 macrophage cell line) was cultured in Eagle's minimal essential medium containing 10% heat-inactivated FBS, penicillin (100 IU/ml), and streptomycin (100 μg/ml). The THP-1 cell line stably transfected with DC-SIGN (THP-1-DC-SIGN) was kindly provided by Vineet N. Kewal Ramani (Model Development Section, HIV Drug Resistance Program, National Cancer Institute, National Institutes of Health) and was maintained in RPMI 1640 supplemented with 10% heat-inactivated FBS under 5% CO_2 at 37°C.

Virus infection. A549, THP-1, THP-1-DC-SIGN, NCI-H292, NL-20, WBC 264-9C, and HL-CZ cells were seeded in 15-ml culture tubes at a density of 1×10^6 cells/ml. Cells were infected with 100 50% tissue culture infective doses ($TCID_{50}$) of SARS-CoV TW1 (10) or CoV-229E (with titers determined in Vero E6 or MRC-5 cells, respectively) and cultured for different periods of time. At different time points after infection, cells were harvested and culture supernatants were collected and stored at −70°C. Cell pellets were resuspended in phosphate-buffered saline (PBS) containing 2% heat-inactivated FBS, and the resuspended cells were placed on multiwell glass slides for immunofluorescence staining. For RNase protection assay, cell pellets were resuspended in TRIzol. Uninfected cells and their culture supernatants were collected and used as controls. Experiments that required handling SARS-CoV were performed in the P3 facility in the National Taiwan University College of Medicine. All procedures were performed according to the Centers for Disease Control and Prevention P3 biosafety guidelines.

Monitoring of virus titer. To monitor SARS-CoV and CoV-229E titers, Vero E6 and MARC-5 cells were seeded at 1×10^4 cells/well in 96-well plates. Two days after seeding, 1:10 serial dilutions (from 10^{-1} to 10^{-8}) of culture supernatants harvested from SARS-CoV- or CoV-229E-infected cell cultures were added to quadruplicate wells. Cytopathic effects were read 3 days later. The $TCID_{50}$ was defined as the dose at which two out of four quadruplicate wells exhibited cytopathic effects.

Immunofluorescence staining. SARS-CoV-infected or control A549, THP-1, THP-1-DC-SIGN, NCI-H292, NL-20, WBC 264-9C, and HL-CZ cells in multiwell slides were air dried and fixed in acetone at −20°C for 15 min. The THP-1, THP-1-DC-SIGN, WBC 264-9C, and HL-CZ cells were first treated with Fc fragments (Chemicon International Inc., Temecula, CA) at a 1:75 dilution to block nonspecific binding to human antibodies through the Fc receptor. To detect SARS-CoV antigen, the cells were then incubated with convalescent-phase sera from confirmed SARS patients (1:25 dilution) at 37°C for 30 min. After incubation, the slides were washed and incubated with fluorescein isothiocyanate (FITC)-conjugated rabbit anti-human immunoglobulin (Ig) (Sigma-Aldrich, St. Louis, MO) at 37°C for 30 min. After three washes, the cells were counterstained with Evans blue.

To detect P-selectin and VCAM-1, acetone-fixed cells were stained with FITC-conjugated anti-P-selectin (clone AK4; BioLegend, San Diego, CA) or anti-VCAM-1 (clone STA; BioLegend, San Diego, CA) at room temperature for 1 h. The slides were counterstained with propidium iodide.

For DC-SIGN staining, acetone-fixed cells were stained with mouse anti-human DC-SIGN antibody (MAb 161; R&D Systems) at room temperature for 1 h. After washing, FITC-conjugated anti-mouse IgG (Sigma-Aldrich) was added and the cells were counterstained with Hoechst H33258 stain (Sigma-Aldrich).

RNA preparation and RT-PCR. Total RNA was extracted from infected as well as uninfected control cells with TRIzol (Invitrogen, Carlsbad, CA). One microgram of total RNA was used for cDNA synthesis with an oligo(dT) primer and SuperScript II reverse transcriptase (Invitrogen, Carlsbad, CA). For reverse transcription-PCR (RT-PCR) analysis, the first-strand cDNA was amplified by PCR (35 cycles for P-selectin and 30 cycles for both VCAM-1 and β-actin); the conditions for amplification were denaturation at 95°C for 30 s, annealing at 56°C for 30 s, and elongation at 72°C for 30 s. The forward and reverse primers used were as follows: P-selectin, 5′-CCAGTGCTTATTGTCAGC-3′ and 5′-CACATTGCAGGCTGGAAT-3′; VCAM-1, 5′-CCCTTGACCGGCTGGAGATT-3′ and 5′-CTGGGGGCAACATTGACATAAAGTG-3′; and β-actin, 5′-CCAGAGCAAGAGAGGCATCC-3′ and 5′-CTGTGGTGGTGAAGCTGAAG-3′.

Quantitative real-time RT-PCR. The SAR1S_AS forward and reverse primers and fluorogenic probe were designed by TaqMan Assay Design (Applied Biosystems, Foster City, CA). The sequences of the forward primer, reverse primer, and probe are 5′-CACACCGTTTCTACAGGTTAGCT-3′ (genome positions 15316 to 15338 of the Urbani strain), 5′-GCCACACATGACCATCTCACTTAAT-3′ (positions 15380 to 15356), and 5′-ACGGTTGCGCACACTCGGT-3′ (positions 15355 to 15339), respectively. A 200-bp product covering this region was generated by using the primers (F1 and R1), the Superscript II one-step RT-PCR system (Invitrogen, San Diego, CA), and the RNA template derived from the SARS-CoV TW1 strain (10). The sequences of the primers F1 and R1 are 5′-CAGAGCCATGCCTAACATGC-3′ (genome positions 15239 to 15258) and 5′-GCATAAGCAGTTGTAGCATC-3′ (positions 15439 to 15420), respectively. RT-PCR conditions were 52°C for 40 min and 94°C for 2 min, followed by 35 cycles of 94°C for 1 min, 60°C for 1 min, and 68°C for 45 s. The product was subsequently cloned into the TA cloning vector (Invitrogen, San Diego, CA) to generate the construct ORF1b/pCRII-TOPO (29). The in vitro-transcribed RNA was purified and quantified to determine the RNA copy number as described previously (29). An aliquot (2 μl) of RNA isolated from the sample and known amounts of the in vitro-transcribed RNA (5 to 50 million copies) were subjected to real-time RT-PCR by using the SAR1S_AS primers and probes and the TaqMan one-step real-time RT-PCR master mix reagent kit (Applied Biosystems). The amplification conditions were 48°C for 30 min and 95°C for 10 min, followed by 45 cycles of 95°C for 15 s and 60°C for 1 min. The ABI Prism 7000 sequence detector was used to analyze the emitted fluorescence during amplification. A positive result is defined by the cycle number required to reach the threshold (cycle threshold value), as described previously (29).

RNase protection assay (RPA). Total RNA from infected as well as uninfected cells was isolated and subjected to cytokine and chemokine mRNA analysis as follows. Multiprobe templates were purchased from BD-PharMingen (San Diego, CA), and the assay was performed according to the manufacturer's instructions. Briefly, radiolabeled RNA probes were generated from the multiprobe templates by using T7 RNA polymerase and a mixture of pooled unlabeled nucleotides and [α-^{32}P]UTP. The probes were hybridized overnight with 10 to 20 μg total RNA and then digested first with RNase mixtures and then with proteinase K. RNase-resistant duplex RNAs were extracted with phenol, precipitated with ammonium acetate, solubilized, and resolved on a 5% sequencing gel. Gels were dried and subjected to autoradiograph and phosphorimage analysis. The expression of each cytokine or chemokine is normalized against the L32 housekeeping genes.

Isolation of peripheral blood leukocytes. Peripheral blood was collected from healthy volunteers by venous puncture. Mononuclear cells were separated from neutrophils and red blood cells on Ficoll-Paque (Amersham-Pharmacia, Uppsala, Sweden) by density gradient centrifugation. The mononuclear cells at the interface were collected. The red blood cells in the pellet were lysed. The neutrophils were then mixed with the mononuclear cells and suspended in RPMI

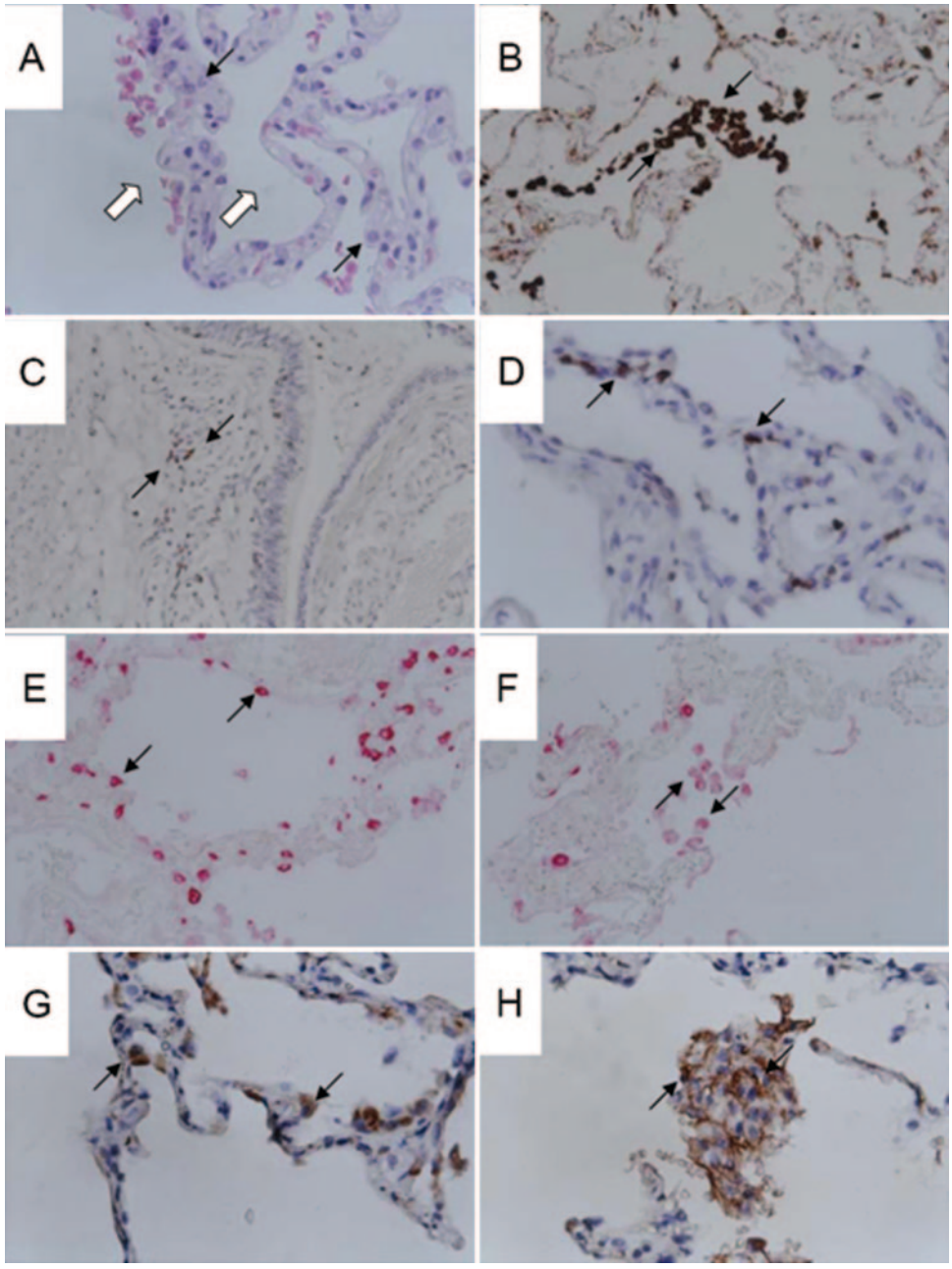

FIG. 1. Histological and immunohistochemical staining of lung sections from a SARS patient at the acute respiratory phase. (A) Hematoxylin-and-eosin staining showing the alveolar structure of a SARS patient who died at day 7 after admission. Solid arrows point to neutrophils in the capillaries of the alveolar septum (magnification, ×400). Open arrows point to empty alveolar spaces. (B) Aggregates of $CD68^+$ macrophages were present in the alveolar space (magnification, ×400). (C) $CD3^+$ T cells were present in the peribronchial stroma and interstitium (magnification, ×200). (D) Scattered mononuclear cells in the alveolar septum were reactive to anti-CD8 antibody (magnification, ×400). (E) SARS-CoV antigen was demonstrated in cuboidal pneumocytes (magnification, ×400). (F) SARS-CoV antigen was demonstrated in alveolar macrophages (magnification, ×400). (G) The alveolar pneumocytes were reactive to anti-P-selectin antibody (magnification, ×400). (H) The alveolar macrophages stained positive for P-selectin (magnification, ×400). Arrows point to positive cells.

1640 containing 0.5% bovine serum albumin and 10 mM HEPES (pH 8). To prepare for activated T cells, peripheral blood mononuclear cells were stimulated with 50 ng/ml phorbol myristate acetate (Sigma-Aldrich) and 0.3 μg/ml ionomycin (Sigma-Aldrich) and incubated at 37°C for 72 h in a 5% CO_2 atmosphere.

Chemotaxis assay. Transwell inserts with a 5-μm pore size fitted in 24-well plates (Corning Costar Corp., Corning, N.Y.) were used for chemotaxis assay. One million peripheral blood leukocytes or activated T cells in 100 μl were loaded into the insert above the well containing 600 μl of culture supernatant collected from uninfected, SARS-CoV-infected, or CoV-229E-infected A549 or THP-1-DC-SIGN cells. For neutralization experiments, the supernatants were preincubated with different concentrations of anti-CXCL8/IL-8, CCL2/MCP-1, and CCL5/RANTES antibody (purchased from Preprotech, Rocky Hill, NJ) singly or in combination for 30 min before addition to the insert. The plates were incubated at 37°C in a CO_2 incubator. After incubation for different periods of time, cells attached to the bottom of the insert were gently washed off and combined with the cells at the lower chamber. The cells were collected in

TABLE 1. SARS-CoV nucleic acid and antigen in human cell lines at day 1 after infection

Cell line	IF[a]	Copies/ml[b]
A549	+	1×10^3
NCI-H292	−	ND[c]
NL-20	−	ND
HL-CZ	−	ND
THP-1	+	2×10^4
THP-1-DC-SIGN	++++	2×10^4
WBC 264-9C	−	ND

[a] IF, immunofluorescence staining with convalescent-phase sera from SARS patients. −, negative; +, weakly positive; ++++, strongly positive.
[b] SARS-CoV-infected cells were collected, and the amount of intracellular positive-sense SARS-CoV RNA was determined by real-time RT-PCR. Copy number was determined based on the linear standard curve obtained from the input positive-sense RNA increased from 2 copies to 2,000,000 copies per reaction.
[c] ND, not detectable.

microtubes and centrifuged at 13,000 × *g* for 30 s. The cell pellets were resuspended in 40 μl PBS. Seven microliters of cell suspension was placed on the wells of multiwell slides. The slides were air dried, fixed in cold acetone at −20°C for 15 min, and stained with Leu's stain. The number of cells was counted under a light microscope at a magnification of ×200. At least five fields in each well were counted. There were three repeats for each experimental condition. The extent of cell migration was expressed as number of cells per field.

Protein chip assay. The Human Cytokine Protein Array I was purchased from Ray Biotech (Norcross, GA) and used according to the manufacturer's instructions. Briefly, membranes were incubated for 30 min in 0.01 M Tris-HCl buffer (pH 7.6) containing 0.15 M NaCl and 5% bovine serum albumin. After incubation, membranes were subjected to three 5-min washes with 1× PBS–0.1% Tween, followed by two 5-min washes with 1× PBS–0.1% Tween. Supernatants from A549 or THP-1-DC-SIGN cell cultures with or without SARS CoV infection were added to the membrane and incubated for 1 h, followed by incubation with biotin-conjugated anti-cytokine/chemokine antibody provided with the kit. The membranes were then washed twice with 1× PBS–0.1% Tween and incubated with horseradish peroxidase-conjugated streptavidin for 30 min. Unbound reagents were washed, and the membranes were developed by ECL as provided in the kit.

Western blotting. Twenty microliters of conditioned supernatants from SARS-CoV-infected cell cultures were subjected to electrophoresis in 10% sodium dodecyl sulfate-polyacrylamide gels. The resolved proteins were transferred onto Hybond P membranes using a semidry transfer system (Amersham Biosciences, Chandler, AZ). The membrane was blocked with PBS containing 5% nonfat milk and 0.1% Tween 20. The membrane was then incubated with 1:1,000 dilution of anti-DC-SIGN (MAb 161; R&D Systems) or antitubulin antibody (DM1A; Sigma-Aldrich) overnight. Blots were washed once for 10 min and three times for 5 min in PBS containing 0.1% Tween 20 and then incubated with horseradish peroxidase-conjugated donkey anti-mouse IgG (Amersham Bioscience) in PBS containing 0.1% Tween 20 for 30 min. The bound antibody was detected using the ECL Plus kit (Amersham Bioscience).

RESULTS

Early events occurring in the lung of a SARS patient. Published reports have demonstrated overwhelming cellular infiltration in patients who died during late-stage SARS-CoV infection (11). However, the events that occurred proceeding severe respiratory distress have not been revealed. To address this question, lung sections from a confirmed SARS patient who died at day 7 after admission to the hospital were examined. Figure 1A shows that the alveolar spaces in the lung section were open with only mild cellular infiltration in the septum, indicating that the patient was at an early stage of disease. The infiltrating cells included neutrophils in the interstitia (Fig. 1A), $CD68^+$ macrophages in the alveolar space (Fig. 1B), and $CD3^+$ T cells in the peribronchial region and interstitia (Fig. 1C). No $CD20^+$ B cells or $CD56^+$ NK cells were seen (data not shown). Interestingly, most of the infiltrating T cells were of the $CD8^+$ (Fig. 1D) but not the $CD4^+$ (data not shown) phenotype. SARS-CoV antigens were present in cells morphologically consistent with pneumocytes (Fig. 1E) as well as macrophages (Fig. 1F), which is consistent with published results (23). In addition, both pneumocytes and macrophages expressed P-selectin (Fig. 1G and H). These results demonstrate the types of cells that were recruited to the lungs of patients during the early stage of SARS. However, the question of what cellular response results in the infiltration of neutrophils, monocytes, and T cells remains to be addressed.

Susceptibility of A549 and THP-1 cells to SARS-CoV infection. Several established human lung epithelial cells lines (A549, NCI-H292, NL-20, and HL-CZ) and monocytic leuke-

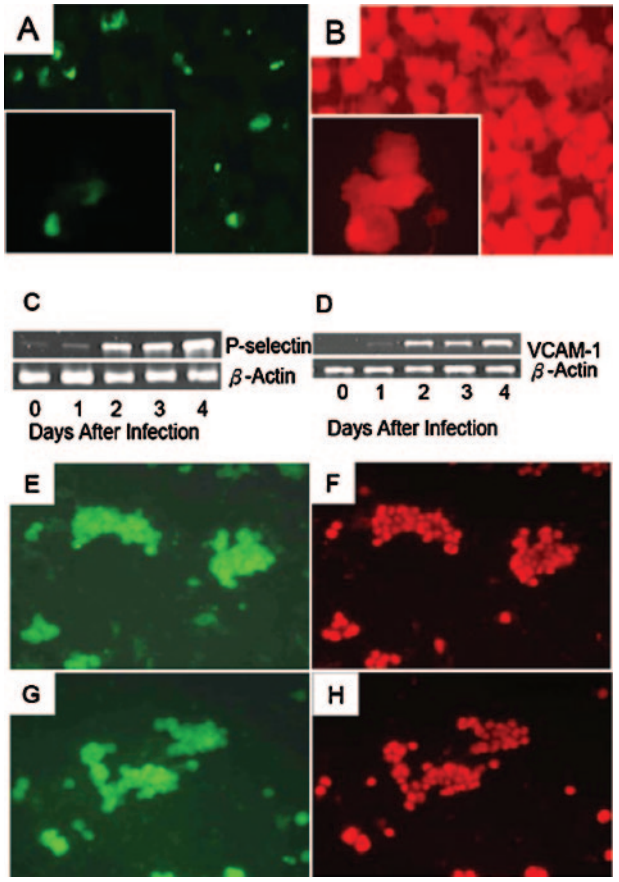

FIG. 2. SARS-CoV infects alveolar epithelial A549 cells and induces expression of P-selectin and VCAM-1. (A and B) A549 cells were inoculated with 100 $TCID_{50}$ of SARS-CoV, harvested at day 7, and incubated with convalescent-phase serum from a SARS patient followed by FITC-conjugated rabbit anti-human Ig antibody. The experiment was repeated using convalescent-phase sera from five different SARS patients, and similar results were obtained. Evans blue was used as a counterstain. Magnification, ×400. Results of one representative experiment are shown. (C and D) At days 1, 2, 3, and 4 after infection, total RNA was extracted and subjected to RT-PCR amplification of the P-selectin (C), VCAM-1 (D), and β-actin (C and D) genes. (E to H) SARS-CoV-infected cells were harvested at day 5 of culture and stained with FITC-conjugated anti-P-selectin (E) or anti-VCAM-1 (G) antibody. Propidium iodide was used as a counterstain (F and H). Original magnification, ×400. The experiment was repeated three times, and results of one representative experiment are shown.

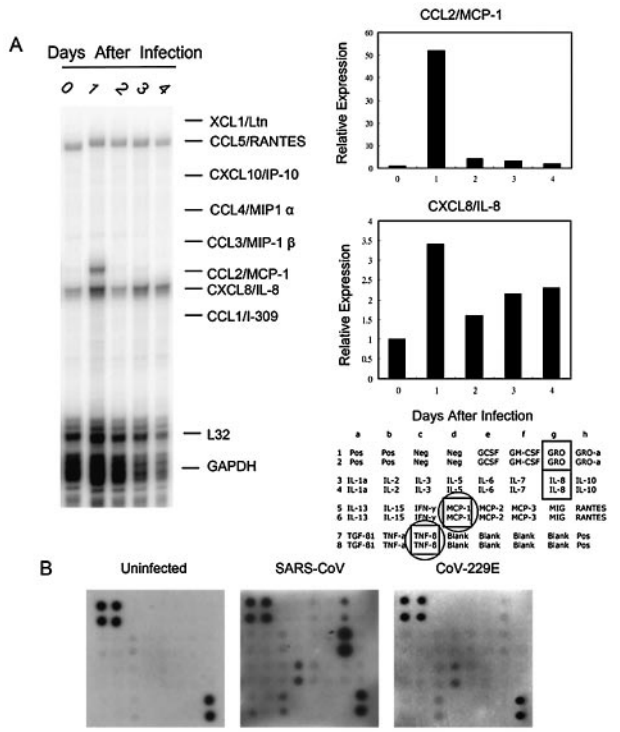

FIG. 3. SARS-CoV induces expression of chemokines in A549 cells. (A) A549 cells were infected with SARS-CoV as described for Fig. 2. At different days after infection, total RNA was extracted and subjected to RPA and phosphorimaging. The intensities of the CCL2/MCP-1 and CXCL8/IL-8 mRNA phosphorimages were normalized against that of the L32 housekeeping gene. The data presented are representative of two independent experiments. (B) The supernatants from uninfected (left panel), SARS-CoV-infected (middle panel), or CoV-299E-infected (right panel) A549 cells were collected at day 1 after infection. The cytokines and chemokines secreted into the supernatants were determined on the protein chip. The positions of cytokines and chemokines on the array are shown. The cytokines/chemokines that were detected in the supernatant of SARS-CoV-infected cells are boxed. Those that were in the supernatant of CoV-229E-infected cells are circled.

mia and macrophage cell lines (THP-1 and WBC 264-9C) were examined for their permissiveness to SARS-CoV infection. Cell lines were infected with 100 $TCID_{50}$ of SARS-CoV. At days 1 and 7 after infection, cells were fixed and stained with SARS patient serum. Before staining, an Fc block was used to block nonspecific binding of human immunoglobulin to Fc receptors on macrophages and monocytic cell lines. Real-time PCR and indirect immunofluorescence staining revealed the presence of SARS-CoV nucleic acid and antigen in A549 and THP-1 cells (Table 1; Fig. 2A), whereas all other cell lines were virus-free (Table 1).

SARS-CoV infection induces pneumocytic epithelial cell production of CCL2/MCP-1 and CXCL8/IL-8 and expression of adhesion molecules. Given that recruitment of leukocytes to the site of inflammation is orchestrated by chemokines and that pneumocytes are resident cells in the lungs and targets of SARS-CoV (16), we next examined whether and how SARS-CoV infection of pneumocytes would influence inflammatory cell recruitment. A549 pneumocytic epithelial cells were infected with SARS-CoV, and their chemokine profile was examined (10). The RPA results show that CCL2/MCP-1 and CXCL8/IL-8 expression in SARS-CoV-infected A549 cells surged at day 1 after infection. The CCL2/MCP-1 mRNA level was 52.2-fold higher than that in uninfected cells, while the CXCL8/IL-8 mRNA level was 3.4-fold higher (Fig. 3A). Their expression decreased by day 2 but remained higher than that in the controls until day 4 of infection.

The finding that the expression of CCL2/MCP-1 and CXCL8/IL-8 mRNAs surged in SARS-CoV-infected A549 cells led us to test whether the corresponding proteins and other cytokines/chemokines also increase. Culture supernatants collected from SARS-CoV-infected cells were compared with CoV 229E-infected and uninfected control culture supernatants in a protein chip assay, as we have determined that the infectivities of SARS-CoV and CoV-229E were comparable in A549 cells (Table 2). Figure 3B shows that SARS-CoV dramatically induced the secretion of CXCL8/IL-8 in A549 cells. Other chemokines, i.e., CCL2/MCP-1, CXCL1/GRO, and tumor necrosis factor beta, were also induced, but to a lesser extent. The production of these chemokines was notably induced in cells infected with SARS-CoV and only weakly induced in those infected with CoV-229E, indicating that SARS-CoV induces a distinct set of chemokines in pneumocytic epithelial cells. While the protein chip assay is not meant to be used for quantitative comparison between different chemokines and cytokines, these results are consistent with those from RPA. Importantly, the RPA and protein chip assay together showed that CCL2/MCP-1 and CXCL8/IL-8 are the most prominent chemokines produced by lung epithelial cells infected with SARS-CoV (Fig. 3A). Furthermore, the results of the chemotaxis assay show that supernatants from SARS-CoV-infected A549 cells induced neutrophil and monocyte but not activated T-cell migration (Fig. 4A). Neutrophil and monocyte migrations were inhibited by antibodies against CXCL8/IL-8 and CCL2/MCP-1, respectively (Fig. 4B). Together, these results demonstrated that SARS-CoV infection of pneumocytic epithelial cells induces CCL2/MCP-1 and CXCL8/IL-8, which mediate the migration of monocytes and neutrophils.

Adhesion molecules, together with chemokines, play a critical role in lymphocyte trafficking to inflammatory sites. Thus, we examined whether adhesion molecules are inducible by SARS-CoV in A549 cells. Immunofluorescence staining demonstrated that almost all the cells in the infected cell cultures, but not those in the uninfected cell cultures, expressed both

TABLE 2. Comparison of SARS-CoV and CoV-229E infectivities in different cell lines[a]

Cell line	Infecting virus	Log_{10} $TCID_{50}$/ml[b]
A549	SARS-CoV	2.5
	CoV-229E	2
THP-1	SARS-CoV	3
	CoV-229E	3
THP-1-DC-SIGN	SARS-CoV	3
	CoV-229E	3

[a] The A549, THP-1, and THP-1-DC-SIGN cell lines were infected with SARS-CoV and CoV-229E virus. The titer of the virus released into culture supernatants was determined in VeroE6 (SARS-CoV) or MRC-5 (CoV-229E) cells.
[b] Log_{10} value of virus dilution at which CPE was observed in half of the quadruplicate wells.

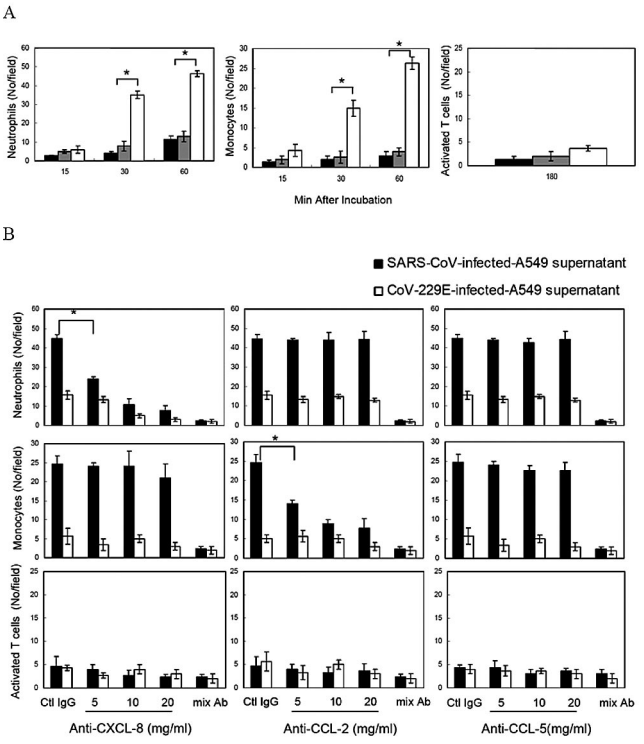

FIG. 4. Chemotactic response of human peripheral blood leukocytes to chemokines secreted by SARS-CoV- or CoV-229E-infected A549 cells. (A) Human peripheral blood leukocytes or activated T cells (1×10^6) were loaded onto inserts in wells containing culture supernatants from uninfected, SARS-CoV-infected, or CoV-229E-infected A549 cells and incubated for 15, 30, or 60 min (peripheral blood leukocytes) or 180 min (activated T cells). After incubation, migrated cells in the wells were collected, counted, and stained with Leu's stain. Neutrophils (left panel), monocytes (middle panel), and activated T cells (right panel) that migrated to the lower chamber after exposure to supernatants from uninfected cells (dark bars), CoV-229E-infected cells (gray bars), and SARS-CoV-infected cells (empty bars) were enumerated. Cell numbers in at least five fields at a magnification of ×200 were counted. The experiment was repeated two times and results of one representative experiment are shown. *, $P < 0.01$; #, $P < 0.05$. (B) Supernatants collected from SARS-CoV- and CoV-229E-infected A549 cells were preincubated with 5, 10, or 20 mg/ml of anti-CXCL8, anti-CCL2, and anti-CCL5 antibodies singly or in combination for 30 min at room temperature before the experiment. The experiment was performed as described for panel A. *, $P < 0.01$. Error bars indicate standard deviations.

P-selectin and VCAM-1 by day 5 after infection (Fig. 2E and G). The RT-PCR results also show that both P-selectin and VCAM-1 mRNAs were induced in A549 cells as early as day 1 and that the levels of expression were high from day 2 to 4 after SARS-CoV infection (Fig. 2C and D). Interestingly, we found that P-selectin was expressed in cells morphologically consistent with pneumocytes as well as alveolar macrophages in patient during early phase of SARS infection (Fig. 1G and H). Therefore, it appears that by infecting pneumocytic epithelial cells, SARS-CoV induces a set of chemokines and adhesion molecules that would support the migration of neutrophils and monocytes to the site of infection.

SARS-CoV interaction with pneumocytic epithelial cells and monocytic cells induces DC-SIGN expression. Given that SARS-CoV antigen could be detected in the intra-alveolar macrophages in the early phase of SARS (Fig. 1F) and that SARS-CoV-infected pneumocytes rapidly generated CCL2/MCP-1 (Fig. 3), we hypothesized that as a result of pneumocyte infection by SARS-CoV, monocytes are recruited to the lungs. We then studied the interactive relationship between monocytic cells and SARS-CoV. Real-time RT-PCR and immunofluorescence staining revealed the presence of SARS-CoV nucleic acid and antigen in monocytic THP-1 cells (Table 1 and Fig. 5A). In addition, THP-1 and SARS-CoV interaction induced DC-SIGN upregulation (Fig. 6E). DC-SIGN was detectable at day 3 and became prominent at days 4 to 5 after infection. The importance of DC-SIGN in monocytic cell interaction with SARS-CoV is further illustrated in Fig. 5A and C. While only a small percentage of THP-1 cells were targeted by SARS-CoV (Fig. 5A), almost all DC-SIGN-transfected THP-1 cells were targeted by the same titer of virus (Fig. 5C). These results demonstrate that expression of DC-SIGN facilitates the interaction between SARS-CoV and monocytic cells. Interestingly, SARS-CoV infection also induced the expression of DC-SIGN in pneumocytic epithelial cells (Fig. 6A). These in vitro experiments suggest that DC-SIGN is inducible in monocytic cells as well as pneumocytic epithelial cells after SARS-CoV infection.

To address whether DC-SIGN expression has any correlation with SARS-CoV infection in vivo, a lung section from a SARS-CoV-infected patient was examined. Figure 6C and D show that cells morphologically consistent with alveolar macrophages and pneumocytes in the SARS patient expressed DC-SIGN. The results from both in vitro experiments and in situ immunohistochemistry indicate that DC-SIGN expression is important to the SARS-CoV–cell interaction.

SARS-CoV-infected monocytic THP-1 cells produce chemokines that attract neutrophils, monocytes, and activated T cells. We next examined the cellular response of monocytic cells to SARS-CoV. The RPA results in Fig. 5E demonstrate that THP-1-DC-SIGN cells expressed multiple chemokines as early as day 1 after SARS-CoV infection. The chemokine mRNA expression with respect to that in uninfected cells was increased as follows: CCL2/MCP-1, 7.1-fold; CXCL8/IL-8, 4.9-fold; CCL3/MIP-1α, 4.6-fold; CXCL10/IP-10, 3.1-fold; CCL4/MIP-1β, 2.1-fold; and CCL5/RANTES, 1.8-fold. Their expression declined on day 2 but remained at the same level until day 3 of infection. Protein chip assay was performed to compare cytokine and chemokine production by SARS-CoV- and CoV-229E-infected THP-1-DC-SIGN cells (Fig. 5F), as the infectivities of SARS-CoV and CoV-229E to THP-1-DC-SIGN cells were comparable (Table 2). The results show that while SARS-CoV-infected THP-1-DC-SIGN cells produced prominent CCL5/RANTES, CXCL8/IL-8, and CCL2/MCP-1, CoV-229E-infected cells produced no CXCL5/RANTES or CCL2/MCP-1 and weak CXCL8/IL-8 and IL-6. Together, these data show that SARS-CoV infection of monocytic cells induces a distinct set of chemokines that attract neutrophils (CXCL8/IL-8), monocytes (CCL2/MCP-1, CCL5/RANTES, CCL3/MIP-1α, and CCL4/MIP-1β), and activated T cells (CCL2/MCP-1, CCL3/MIP-1α, CCL5/RANTES, and CXCL10/IP-10).

Chemotaxis assay was then performed to compare the effects of SARS-CoV and CoV-229E infection of monocytic cells on cell migration. Figure 7A shows that monocyte and neutrophil migration was significantly greater when peripheral blood leukocytes were exposed to culture supernatant from SARS-CoV-infected

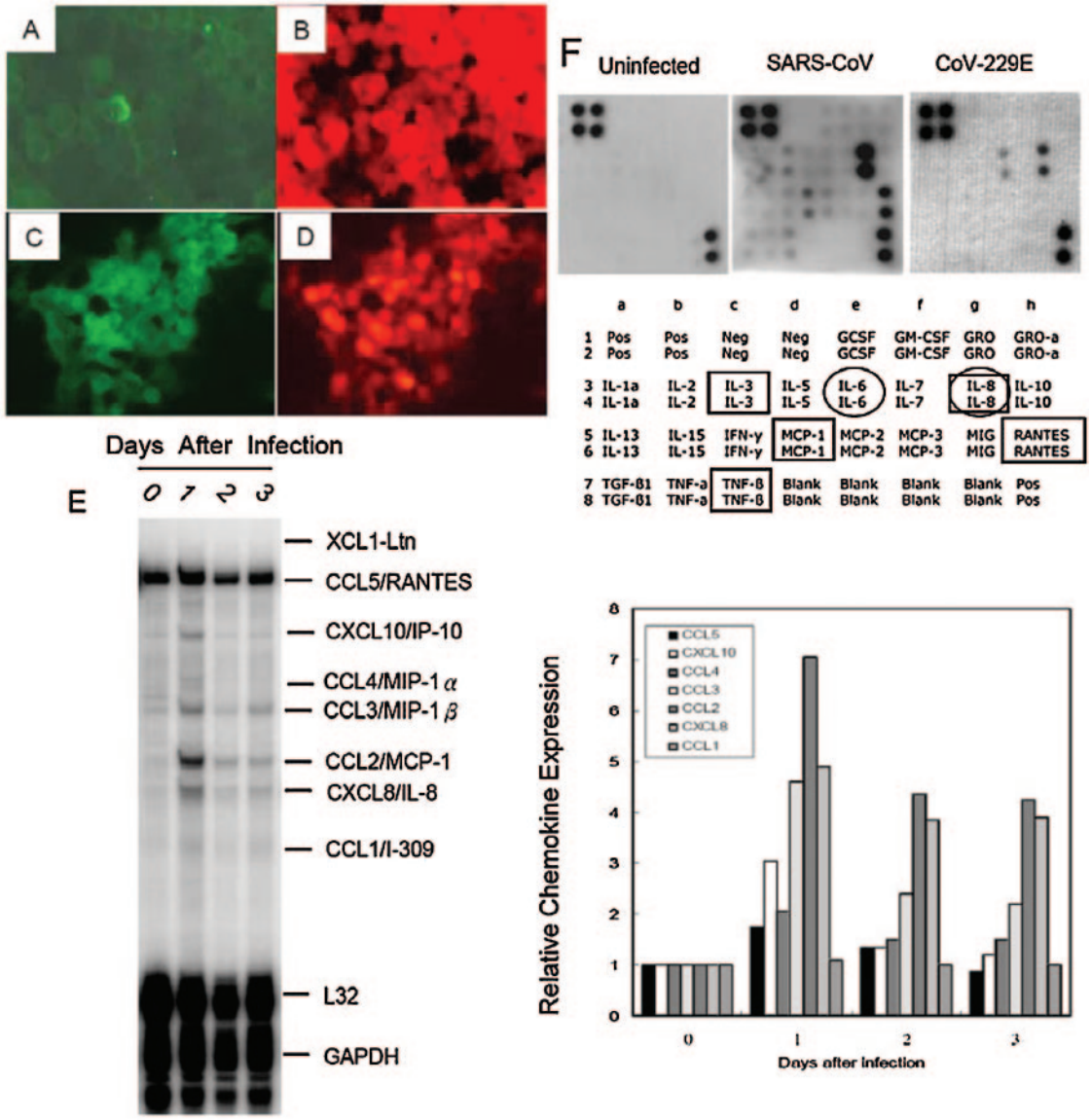

FIG. 5. SARS-CoV infection of monocytic cells induces chemokine expression. (A to D) THP-1 (A and B) and THP-1-DC-SIGN (C and D) cells were infected with SARS-CoV at 100 $TCID_{50}$. At day 5 after infection, cells were harvested and placed on multiwell slides. After fixation and air drying, the cells were first treated with Fc fragment for 30 min and washed before application of convalescent-phase SARS patient serum (A and C), followed by FITC-conjugated rabbit anti-human Ig. Evans blue was used as a counterstain (B and D). Original magnification, ×400. (E) Total RNA was extracted and subjected to RPA as described for Fig. 3. The results shown are representative of three independent experiments. The bar graph shows the relative expression levels of each chemokine with respect to that of the L32 housekeeping gene. (F) Protein arrays show the cytokines and chemokines secreted by uninfected (left panel), SARS-CoV-infected (middle panel), or CoV-299E-infected (right panel) THP-1-DC-SIGN cells into culture supernatants at 1 day after incubation. The results shown are representative of two independent experiments. The cytokines/chemokines that were detected in the supernatant of SARS-CoV-infected cells are boxed. Those that were in the supernatant of CoV-229E-infected cells are circled.

cells than when they were exposed to CoV-229E-infected cells. The difference was detectable at as early as 30 min, and the difference became greater at 60 min after exposure. After a 3-h chemotaxis assay, migration of activated T cells exposed to culture supernatants from SARS-CoV-infected cells was significantly greater than that of cells exposed to supernatants from uninfected or CoV-229E-infected cells. Furthermore, neutrophil migration was inhibited by anti-CXCL8/IL-8 antibody; monocyte migration was inhibited by anti-CCL2/MCP-1 and anti-CCL5/RANTES antibodies; and activated T-cell migration was inhibited by anti-CXCL-8/IL-8, anti-CCL2/MCP-1, and anti-CCL5/RANTES antibodies (Fig. 7B). These chemotaxis results demonstrate that SARS-CoV but not CoV-229E induces the production of chemokines that are functionally active in recruiting neutrophils, monocytes, and activated T cells.

DISCUSSION

The typical acute respiratory phase of SARS, characterized by mild respiratory symptoms and fever, starts at 2 to 7 days

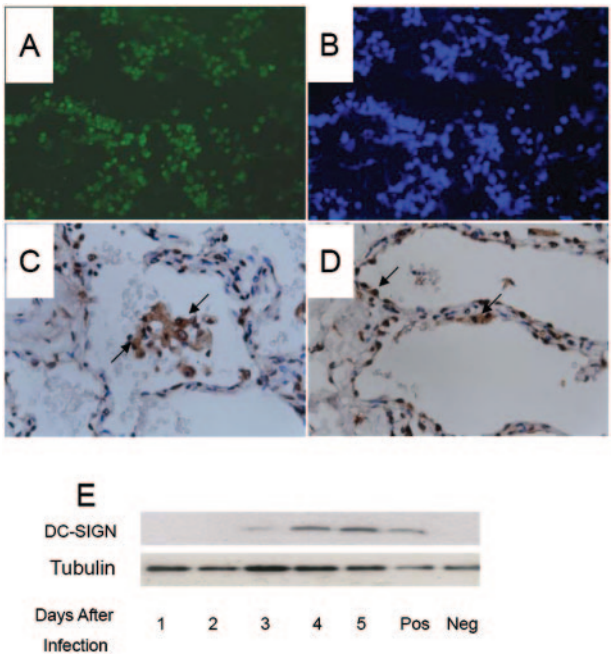

FIG. 6. DC-SIGN expression in SARS-CoV-infected alveolar epithelial cells and in the lung section from a SARS patient. (A and B) SARS-CoV-infected A549 cells were harvested at day 5 after infection and incubated with mouse anti-human DC-SIGN antibody followed by FITC-conjugated anti-mouse IgG (A). Hoechst H33258 was used as counterstain (B). (C and D) Immunohistochemical staining of a lung section from a SARS patient reveals that cells morphologically consistent with alveolar macrophages (C) and pneumocytes (D) are DC-SIGN positive. Magnification for C and D, ×400. Arrows in C and D point to positive cells. (E) At different time points after infection, proteins from THP-1 cells were extracted and subjected to Western blot analysis for DC-SIGN and tubulin. The results shown are representative of three independent experiments.

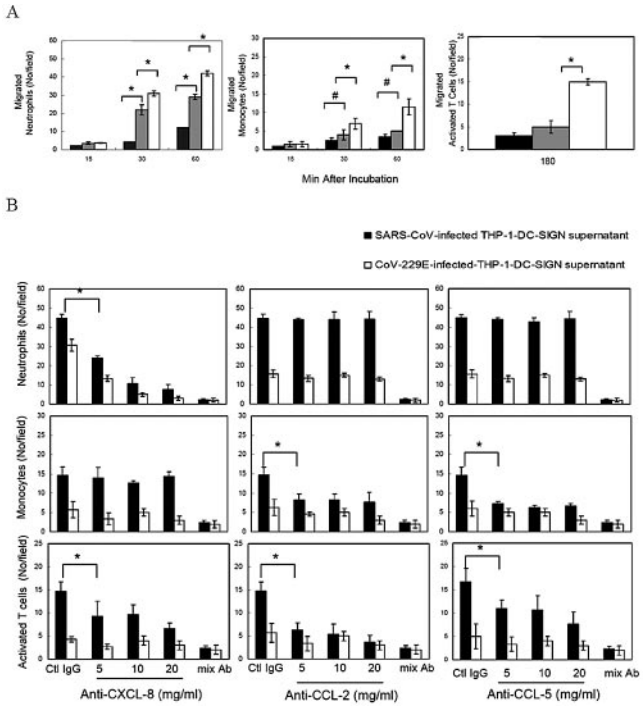

FIG. 7. Chemotactic response of human peripheral blood leukocytes to chemokines secreted by SARS-CoV- or CoV-229E-infected THP-1-DC-SIGN cells. (A) Human peripheral blood leukocytes or activated T cells (1×10^6) were exposed to culture supernatants from uninfected, SARS-CoV-infected, or CoV-229E-infected THP-1-DC-SIGN cells, and the experiment was done as described in the legend to Fig. 4A. The migration of neutrophils (left panel), monocytes (middle panel), and activated T cells (right panel) to the lower chamber after exposure to supernatants from uninfected cells (dark bars), CoV-229E-infected cells (gray bars), and SARS-CoV-infected cells (empty bars) were enumerated. Cell numbers in at least five fields at a magnification of ×200 were counted. The experiment was repeated three times, and results of one representative experiment are shown. *, $P < 0.01$; #, $P < 0.05$. (B) Supernatants collected from SARS-CoV- and CoV-229E-infected THP-1-DC-SIGN cells were preincubated with 5, 10, or 20 mg/ml of anti-CXCL8, anti-CCL2, and anti-CCL5 antibodies singly or in combination for 30 min at room temperature before the experiment. The experiment was performed as described for Fig. 4A. *, $P < 0.01$. Error bars indicate standard deviations.

after onset of symptoms and lasts about 1 to 10 days (3). Most cases progress to the late respiratory phase, which is characterized by moderate to severe respiratory symptoms with dyspnea and hypoxia. Early-phase chest radiographs often show subtle peripheral pulmonary infiltrates (3, 15, 27). The respiratory tracts of affected individuals who die during the first 10 days of illness show diffuse alveolar damage with a mixed alveolar infiltrate, lung edema, and hyaline membrane formation (1). Macrophages are a prominent component of the cellular exudates in the alveoli and lung interstitium (1, 5, 16). Our study reveals that cellular infiltrates in the acute phase of SARS include macrophages, neutrophils, and $CD8^+$ T cells.

Analysis of lung tissues from the SARS-CoV-infected patient who died at late phase showed excessive recruitment of leukocytes, indicating that chemokines play a key role in the pathogenesis of SARS-CoV infection. In addition, immunohistochemistry, in situ hybridization, and electron microscopy on autopsy or tissue biopsy showed that SARS-CoV replicates in pneumocytes and macrophages (18, 23). To investigate the chemokines that are involved in cellular infiltration, we first established that A549 and THP-1 cells are susceptible to SARS-CoV infection (Table 1), although A549 has been reported to be a poor host cell for SARS-CoV replication (6, 13). Our in vitro culture systems showed that A549 cells infected with SARS-CoV produce CCL2/MCP-1 and CXCL8/IL-8 as early as day 1 after infection. We hypothesized that monocytes and neutrophils are the first wave of cells recruited to the lungs after SARS-CoV infection. As monocytic cells are also targets for SARS-CoV, it was important to examine their responses to the virus. Monocytic cells infected by SARS-CoV but not CoV-229E express CCL2/MCP-1, CXCL8/IL-8, CCL3/MIP-1α, CCL5/RANTES, and CXCL10/IP-10 (Fig. 5E and F). Chemotaxis assay showed that neutrophils, monocytes, and activated T cells are recruited (Fig. 7). Therefore, it is possible that after interaction with SARS-CoV, the recruited macrophages produce chemokines that attract a second wave of cells which include monocytes, neutrophils, and activated T cells. Since the macrophages are targets for SARS-CoV, they become another source of chemokines to recruit more immune cells. Thus, alveolar consolidation and eventual lung injury may be the results of accumulation of overwhelming numbers of immune cells and repeated cycles of chemokine production and cell recruitment.

Our study showed that both epithelial and monocytic cells are induced to express high levels of CCL2/MCP-1 after SARS-CoV infection. Since CCL2/MCP-1 is a potent chemoattractant for monocytes, its production by infected cells may be vital to the immunopathogenic mechanism of SARS (19). It has been reported that bronchial lavage fluid from patients with ARDS contain high levels of CCL2/MCP-1, in addition to the presence of CXCL8/IL-8 (4, 21). An overwhelming presence of alveolar monocytes/macrophages is the characteristics of ARDS, and the CCL2/MCP-1 levels in ARDS patients correlate with the severity of lung injury (22). The mortality of infection-induced ARDS is directly related to high CCL2/MCP-1 levels during the early phase of infection (7). Since the clinical symptoms of SARS resemble those of ARDS, one can speculate that the levels of CCL2/MCP-1 expression by SARS-CoV-infected pulmonary epithelial and monocytic cells may also correlate with the severity of SARS. Experimental intratracheal instillation of CCL2/MCP-1 in animals induces localization of monocytes into the alveolar space within 48 h (14). Besides causing chemotaxis, CCL2/MCP-1 also induces calcium influx and production of oxygen radicals and superoxide anion by monocytes (20). It is therefore suggested that monocyte influx in ARDS contributes to lung injury, which is developed in the early as well as the late fibroproliferative phase of the inflammatory disorder (8, 17, 22). Our results showing high levels of CCL2/MCP-1 production by both SARS-CoV-infected epithelial and monocytic cells indicate that the immunopathogenesis of SARS resembles that of ARDS and that CCL2/MCP-1 is important to lung injury.

Our in vitro experiments showed that A549 cells infected with SARS-CoV express the adhesion molecules P-selectin and VCAM-1 (Fig. 2). It has recently been reported that P-selectin is expressed in mouse tissue macrophages and that P-selectin mediates macrophage homotypic interaction (25). Our study demonstrated for the first time that pneumocytes and alveolar macrophages in lung tissue of a SARS patient express P-selectin (Fig. 1G and H). It is plausible that by inducing the expression of adhesion molecules, SARS-CoV infection of lung epithelial cells creates a microenvironment that is conducive for monocyte and neutrophil influx and alveolar macrophage aggregate formation.

It has recently been shown that pseudotype virus containing SARS-CoV spike protein binds to DC-SIGN but does not productively infect DC-SIGN-transfected cells (31). In our in vitro studies, viable SARS-CoV induced DC-SIGN expression in epithelial cells as well as in monocytic cells (Fig. 6A and E). Moreover, almost all monocytic THP-1 cells stably transfected with DC-SIGN bound SARS-CoV although THP-1-DC-SIGN did not increase the SARS-CoV mRNA copy number (Table 1). These results demonstrate that there is a dynamic relationship between SARS-CoV infection and DC-SIGN expression. Immunohistochemical staining revealed that alveolar macrophages and pneumocytes in the lung of SARS patients express DC-SIGN (Fig. 6C and D). In mapping the tissue expression of DC-SIGN, Soilleux et al. showed that interstitial alveolar macrophages but not pneumocytes in histologically normal adult lung tissue constitutively express DC-SIGN and that peripheral blood monocytes are DC-SIGN-negative (24). It is our speculation that DC-SIGN expression on pneumocytes of SARS patients is induced by the virus and that on alveolar macrophages is a combination of both constitutive and inducible expression. By increasing DC-SIGN expression on pneumocytes and monocytes, the dynamics of the SARS-CoV interaction with cells increases and more severe consequences result. DC-SIGN-positive macrophages capturing and transmitting SARS-CoV may play a role in promoting pneumocyte infection.

Although the hypothesis needs to be tested in an animal model, based on our in situ staining and in vitro experiments comparing SARS-CoV and CoV-229E, we propose that the distinct events following SARS-CoV infection that lead to severe respiratory illness in the lungs are as follows. (i) SARS-CoV infects pneumocytes. (ii) Infected pneumocytes produce CCL2/MCP-1 and CXCL8/IL-8 and express P-selectin and VCAM-1 on the surface, providing an environment that is conducive to monocyte and neutrophil migration. (iii) Recruited monocytes interacting with SARS-CoV through DC-SIGN transmit and promote infection of more pneumocytes. (iv) As a result of their interaction with SARS-CoV, the recruited monocytes produce a distinct set of chemokines that recruit more neutrophils (CXCL8/IL-8), monocytes (CCL2/MCP-1, CCL3/MIP-1α, CCL4/MIP-1β, and CCL5/RANTES), and activated T cells (CCL2/MCP-1, CCL3/MIP-1α, CCL5/RANTES, CXCL10/IP-10, and CXCL8/IL-8). As CCL2/MCP-1 is one of the most prominent chemokines produced by SARS-CoV-infected epithelial and monocytic cells and is the key chemokine that causes lung injury in ARDS, our results offer an explanation for the clinical resemblance of SARS to ARDS.

ACKNOWLEDGMENTS

This work was supported by grants NSC92-2751-B002-009-Y and NSC92-3112-B002-039 from the National Science Council, ROC.

We gratefully acknowledge Shu-Chin Chen for helpful discussion and thank Chao-Szu Wu and Hue-Ju Yang for technical assistance.

REFERENCES

1. **Chen, J., Y. Q. Xie, H. T. Zhang, J. W. Wan, D. T. Wang, Z. H. Lu, Q. Z. Wang, X. H. Xue, W. X. Si, Y. F. Luo, and H. M. Qiu.** 2003. Lung pathology of severe acute respiratory syndrome. Zhongguo Yi Xue Ke Xue Yuan Xue Bao **25:**360–362.
2. **Chen, P. C., and C. H. Hsiao.** 2004. Letter. J. Pathol. **203:**729–731.
3. **Christian, M. D., M. Loutfy, L. C. McDonald, K. F. Martinez, M. Ofner, T. Wong, T. Wallington, W. L. Gold, B. Mederski, K. Green, and D. E. Low.** 2004. Possible SARS coronavirus transmission during cardiopulmonary resuscitation. Emerg. Infect. Dis. **10:**287–293.
4. **Donnelly, S. C., R. M. Strieter, S. L. Kunkel, A. Walz, C. R. Robertson, D. C. Carter, I. S. Grant, A. J. Pollok, and C. Haslett.** 1993. Interleukin-8 and development of adult respiratory distress syndrome in at-risk patient groups. Lancet **341:**643–647.
5. **Franks, T. J., P. Y. Chong, P. Chui, J. R. Galvin, R. M. Lourens, A. H. Reid, E. Selbs, C. P. McEvoy, C. D. Hayden, J. Fukuoka, J. K. Taubenberger, and W. D. Travis.** 2003. Lung pathology of severe acute respiratory syndrome (SARS): a study of 8 autopsy cases from Singapore. Hum. Pathol. **34:**743–748.
6. **Gillim-Ross, L., J. Taylor, D. R. Scholl, J. Ridenour, P. S. Masters, and D. E. Wentworth.** 2004. Discovery of novel human and animal cells infected by the severe acute respiratory syndrome coronavirus by replication-specific multiplex reverse transcription-PCR. J. Clin. Microbiol. **42:**3196–3206.
7. **Goodman, R. B., R. M. Strieter, D. P. Martin, K. P. Steinberg, J. A. Milberg, R. J. Maunder, S. L. Kunkel, A. Walz, L. D. Hudson, and T. R. Martin.** 1996. Inflammatory cytokines in patients with persistence of the acute respiratory distress syndrome. Am. J. Respir. Crit. Care Med. **154:**602–611.
8. **Headley, A. S., E. Tolley, and G. U. Meduri.** 1997. Infections and the inflammatory response in acute respiratory distress syndrome. Chest **111:**1306–1321.
9. **Hsiao, C. H., M. Z. Wu, S. W. Hsieh, L. C. Chien, K. C. Hwang, and I. J. Su.** 2004. Clinicopathology of severe acute respiratory syndrome: an autopsy case report. J. Formosa Med. Assoc. **103:**787–792.
10. **Hsueh, P. R., C. H. Hsiao, S. H. Yeh, W. K. Wang, P. J. Chen, J. T. Wang, S. C. Chang, C. L. Kao, and P. C. Yang.** 2003. Microbiologic characteristics, serologic responses, and clinical manifestations in severe acute respiratory syndrome, Taiwan. Emerg. Infect. Dis. **9:**1163–1167.
11. **Jiang, Y., J. Xu, C. Zhou, Z. Wu, S. Zhong, J. Liu, W. Luo, T. Chen, Q. Qin, and P. Deng.** 2005. Characterization of cytokine/chemokine profiles of severe acute respiratory syndrome. Am. J. Respir. Crit. Care Med. **171:**850–857.

12. **Lee, N., D. Hui, A. Wu, P. Chan, P. Cameron, G. M. Joynt, A. Ahuja, M. Y. Yung, C. B. Leung, K. F. To, S. F. Lui, C. C. Szeto, S. Chung, and J. J. Sung.** 2003. A major outbreak of severe acute respiratory syndrome in Hong Kong. N. Engl. J. Med. **348:**1986–1994.
13. **Li, D., N. Wu, H. Yao, A. Bader, N. H. Brockmeyer, and P. Altmeyer.** 2005. Association of RANTES with the replication of severe acute respiratory syndrome coronavirus in THP-1 cells. Eur. J. Med. Res. **10:**117–120.
14. **Maus, U., S. Herold, H. Muth, R. Maus, L. Ermert, M. Ermert, N. Weissmann, S. Rosseau, W. Seeger, F. Grimminger, and J. Lohmeyer.** 2001. Monocytes recruited into the alveolar air space of mice show a monocytic phenotype but upregulate CD14. Am. J. Physiol. Lung Cell Mol. Physiol. **280:**L58–L68.
15. **Moore, S. A., R. M. Strieter, M. W. Rolfe, T. J. Standiford, M. D. Burdick, and S. L. Kunkel.** 1992. Expression and regulation of human alveolar macrophage-derived interleukin-1 receptor antagonist. Am. J. Respir. Cell Mol. Biol. **6:**569–575.
16. **Nicholls, J. M., L. L. Poon, K. C. Lee, W. F. Ng, S. T. Lai, C. Y. Leung, C. M. Chu, P. K. Hui, K. L. Mak, W. Lim, K. W. Yan, K. H. Chan, N. C. Tsang, Y. Guan, K. Y. Yuen, and J. S. Peiris.** 2003. Lung pathology of fatal severe acute respiratory syndrome. Lancet **361:**1773–1778.
17. **Openshaw, P. J.** 2004. What does the peripheral blood tell you in SARS? Clin. Exp. Immunol. **136:**11–12.
18. **Peiris, J. S., C. M. Chu, V. C. Cheng, K. S. Chan, I. F. Hung, L. L. Poon, K. I. Law, B. S. Tang, T. Y. Hon, C. S. Chan, K. H. Chan, J. S. Ng, B. J. Zheng, W. L. Ng, R. W. Lai, Y. Guan, and K. Y. Yuen.** 2003. Clinical progression and viral load in a community outbreak of coronavirus-associated SARS pneumonia: a prospective study. Lancet **361:**1767–1772.
19. **Rollins, B. J.** 1996. Monocyte chemoattractant protein 1: a potential regulator of monocyte recruitment in inflammatory disease. Mol. Med. Today **2:**198–204.
20. **Rollins, B. J., A. Walz, and M. Baggiolini.** 1991. Recombinant human MCP-1/JE induces chemotaxis, calcium flux, and the respiratory burst in human monocytes. Blood **78:**1112–1116.
21. **Rose, C. E., Jr., S. S. Sung, and S. M. Fu.** 2003. Significant involvement of CCL2 (MCP-1) in inflammatory disorders of the lung. Microcirculation **10:**273–288.
22. **Rosseau, S., P. Hammerl, U. Maus, H. D. Walmrath, H. Schutte, F. Grimminger, W. Seeger, and J. Lohmeyer.** 2000. Phenotypic characterization of alveolar monocyte recruitment in acute respiratory distress syndrome. Am. J. Physiol. Lung Cell Mol. Physiol. **279:**L25–L35.
23. **Shieh, W. J., C. H. Hsiao, C. D. Paddock, J. Guarner, C. S. Goldsmith, K. Tatti, M. Packard, L. Mueller, M. Z. Wu, P. Rollin, I. J. Su, and S. R. Zaki.** 2005. Immunohistochemical, in situ hybridization, and ultrastructural localization of SARS-associated coronavirus in lung of a fatal case of severe acute respiratory syndrome in Taiwan. Hum. Pathol. **36:**303–309.
24. **Soilleux, E. J., L. S. Morris, G. Leslie, J. Chehimi, Q. Luo, E. Levroney, J. Trowsdale, L. J. Montaner, R. W. Doms, D. Weissman, N. Coleman, and B. Lee.** 2002. Constitutive and induced expression of DC-SIGN on dendritic cell and macrophage subpopulations in situ and in vitro. J. Leukoc. Biol. **71:**445–457.
25. **Tchernychev, B., B. Furie, and B. C. Furie.** 2003. Peritoneal macrophages express both P-selectin and PSGL-1. J. Cell Biol. **163:**1145–1155.
26. **To, K. F., J. H. Tong, P. K. Chan, F. W. Au, S. S. Chim, K. C. Chan, J. L. Cheung, E. Y. Liu, G. M. Tse, A. W. Lo, Y. M. Lo, and H. K. Ng.** 2004. Tissue and cellular tropism of the coronavirus associated with severe acute respiratory syndrome: an in-situ hybridization study of fatal cases. J. Pathol. **202:**157–163.
27. **Villard, J., F. Dayer-Pastore, J. Hamacher, J. D. Aubert, S. Schlegel-Haueter, and L. P. Nicod.** 1995. GRO alpha and interleukin-8 in Pneumocystis carinii or bacterial pneumonia and adult respiratory distress syndrome. Am. J. Respir. Crit. Care Med. **152:**1549–1554.
28. **Wang, J. T., W. H. Sheng, C. T. Fang, Y. C. Chen, J. L. Wang, C. J. Yu, S. C. Chang, and P. C. Yang.** 2004. Clinical manifestations, laboratory findings, and treatment outcomes of SARS patients. Emerg. Infect. Dis. **10:**818–824.
29. **Wang, W. K., S. Y. Chen, I. J. Liu, Y. C. Chen, H. L. Chen, C. F. Yang, P. J. Chen, S. H. Yeh, C. L. Kao, L. M. Huang, P. R. Hsueh, J. T. Wang, W. H. Sheng, C. T. Fang, C. C. Hung, S. M. Hsieh, C. P. Su, W. C. Chiang, J. Y. Yang, J. H. Lin, S. C. Hsieh, H. P. Hu, Y. P. Chiang, P. C. Yang, and S. C. Chang.** 2004. Detection of SARS-associated coronavirus in throat wash and saliva in early diagnosis. Emerg. Infect. Dis. **10:**1213–12139.
30. **Wong, C. K., C. W. Lam, A. K. Wu, W. K. Ip, N. L. Lee, I. H. Chan, L. C. Lit, D. S. Hui, M. H. Chan, S. S. Chung, and J. J. Sung.** 2004. Plasma inflammatory cytokines and chemokines in severe acute respiratory syndrome. Clin. Exp. Immunol. **136:**95–103.
31. **Yang, Z. Y., Y. Huang, L. Ganesh, K. Leung, W. P. Kong, O. Schwartz, K. Subbarao, and G. J. Nabel.** 2004. pH-dependent entry of severe acute respiratory syndrome coronavirus is mediated by the spike glycoprotein and enhanced by dendritic cell transfer through DC-SIGN. J. Virol. **78:**5642–5650.